Liquid Crystals
Publication details, including instructions for authors and subscription information:
http://www.informaworld.com/smpp/title~content=t713926090

Re-entrant and induced mesophases: Mixed systems showing re-entrant TGB_A and re-entrant cholesteric phases

Volkmar Vill[a]; Hanns-Walter Tunger[a]; Daniel Peters[a]
[a] Institute of Organic Chemistry, University of Hamburg, Hamburg, Germany

To cite this Article Vill, Volkmar , Tunger, Hanns-Walter and Peters, Daniel(1996) 'Re-entrant and induced mesophases: Mixed systems showing re-entrant TGB_A and re-entrant cholesteric phases', Liquid Crystals, 20: 5, 547 — 552

To link to this Article: DOI: 10.1080/02678299608031141

URL: http://dx.doi.org/10.1080/02678299608031141

LIQUID CRYSTALS, 1996, VOL. 20, NO. 5, 547–552

Re-entrant and induced mesophases: Mixed systems showing re-entrant TGB_A and re-entrant cholesteric phases

by VOLKMAR VILL*, HANNS-WALTER TUNGER and DANIEL PETERS
Institute of Organic Chemistry, University of Hamburg, Martin-Luther-King-Platz 6, D-20146 Hamburg, Germany

(Received 27 September 1995; accepted 9 December 1995)

We have investigated the behaviour of chiral carbohydrate-based trioxadecalines with a cyano group in mixed systems. The mixture of a trioxadecaline having a Ch phase and a trioxadecaline having a Ch, S_A and a S_C^* phase sequence induces a re-entrant TGB_A and Ch phase. Below the stabilized S_C^* phase, a re-entrant Ch phase is observed. In the mixture of the cholesteric trioxadecaline with CCH7, itself only showing a nematic phase, a TGB_A phase and a broad range S_A phase are induced from two non-smectic compounds. Both mixtures show a blue phase with a pitch ranging from the UV to red depending on the molar fraction.

1. Introduction

Since the discovery of the TGB_A phase by Goodby *et al.* in 1989 [1], academic interest in chiral mesogens and twisted smectic phases has grown. In most cases, the TGB_A phase occurs at the transition of a cholesteric to a smectic A phase when the molecules try to form a helical structure with the cholesteric helical axis perpendicular to the long axes of the molecules and also try to form a lamellar smectic A structure. A few compounds having a re-entrant cholesteric or nematic phase have been reported [2–4] where the molecules contain a cyano group and form a cholesteric from a smectic A phase. At lower temperatures, the molecules tend to dimerize to minimize the effect of the molecular dipole, but the dimers sometimes prefer to form a cholesteric phase, and so a less ordered cholesteric phase occurs below a higher ordered smectic A phase. However, if a compound exhibits a TGB_A phase at the cholesteric–smectic A interface and shows a re-entrant cholesteric phase, it should also be able to show a re-entrant TGB_A phase.

We recently reported the first observation of a re-entrant TGB_A phase shown by a pure compound ((1S,6R,8R)-8-(4′-undecoxyphenyl)-3-(4″-cyanophenyl)-2,4,7-trioxa-3-bora-bicyclo[4.4.0]decane, CN-B-11). In contact preparations, other members of this homologous series showed the stabilization of the re-entrant phases and the induction of smectic phases from compounds showing no smectic phase by themselves [5]. We continued the research on this matter and investigated the mesomorphic behaviour of mixed systems of the compounds with a defined concentration of the components, and also studied further contact preparations with other components.

2. Experimental

CN-B-10 [5] and CN-C-12 [6] were synthesized as described in [7]. CCH7 was a gift from E. Merck, Darmstadt. HOPDOB [8] and C7-Chol [9] are known compounds. The mesomorphic properties and molecular structures are shown in the table. The mixed systems were prepared by the weighing and mixing method. The compounds were weighed and intensively mixed, giving a series of mixtures with 10 wt % concentration steps (see figures 1 and 2). Contact preparations were made in the usual manner from the two molten samples between a glass slide and cover slip, and the effect of the concentration gradient in the sample was observed microscopically (figure 5).

An Olympus BH optical polarizing microscope equipped with a Mettler FP 82 hot stage and a Mettler FP 80 central processor was used to obtain the phase diagrams. The mesophases were identified by their characteristic textures. The phase diagrams are shown in figures 1 and 2, where the *x* axis represents the molar fraction of CN-B-10.

3. Results and discussion

The mixed system CN-B-10/CCH7 shows the induction of a smectic A phase between two non-smectic compounds (figure 1). On the left-hand side of the diagram, the nematic phase of pure CCH7 is represented, and on the right-hand side, the cholesteric phase of pure CN-B-10.

---

*Author for correspondence.

Structures and mesomorphic properties of the pure compounds.

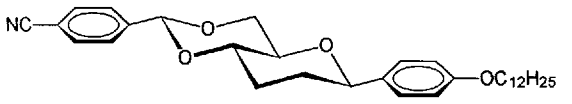

CN-C-12: Cr 105.9 (S_C^* 25) S_A 152.7 Ch 157.2 I

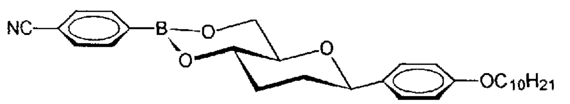

CN-B-10: Cr 104.0 Ch 168.9 (BP) I

CCH7: Cr 71 N 83 I

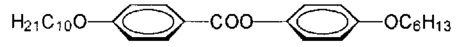

HOPDOB: Cr 62.5 S_C 77.5 S_A 83.3 N 88.9 I

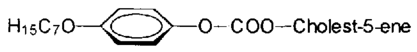

C7-Chol: Cr 113 S_A 133.7 Ch 139 I

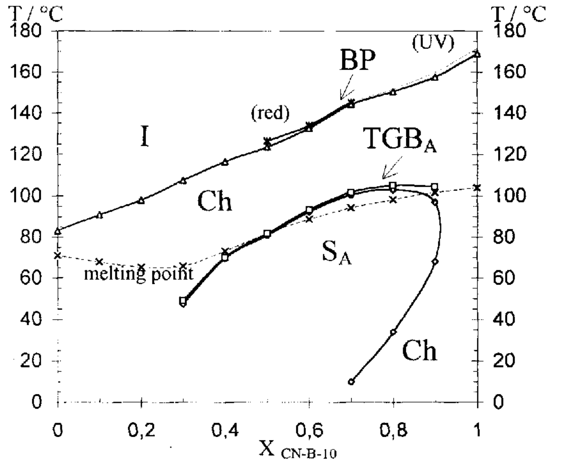

Figure 1. Phase diagram of the mixed system CN-B-10/CCH7.

A small amount of the chiral compound added to nematic CCH7 causes the formation of a chiral nematic phase which is observed for all concentrations containing CN-B-10. Below the cholesteric phase, in the region of 30 to 90 wt % of CN-B-10, a largely monotropic smectic A phase is induced with the highest transition temperature being realized for 80 wt % CN-B-10. No direct transition of the homeotropic smectic A phase to the cholesteric phase is observable. For all concentrations, a TGB$_A$ phase is formed between the smectic A and cholesteric phases, represented by its typical filament texture. As noted in the introduction, a re-entrant TGB$_A$ phase should be observable when a re-entrant cholesteric phase is formed on cooling a S_A phase and the smectic A–cholesteric transition occurs via a TGB$_A$ phase. In this mixed system, for 70 to 90 wt % CN-B-10, a re-entrant cholesteric phase is observed, but no re-entrant TGB$_A$ phase is in fact formed. The interaction of the chiral CN-B-10 and the achiral CCH7 at lower temperatures probably forms molecular aggregates with a lower twisting power than the components of the monomeric mixture at higher temperatures. This would explain the occurrence of a TGB$_A$ phase at higher temperatures, but not at lower temperatures.

For concentrations higher than 40 wt % CN-B-10 a blue phase is observed. At 50 to 70 wt % CN-B-10, the typical platelet texture of the blue phase is exhibited with a remarkable concentration-dependent change of the colour of the platelets; at 50 wt %, the texture is yellowish and red, and with increasing content of the chiral component it changes progressively to blue. The change in colour of the texture represents a pitch change of the blue phase correlating with the wavelength of the light ranging from red through green to blue and then into the UV. A blue phase with a pitch in the UV like that observed for more than 80 wt % of CN-B-10 cannot be detected in the usual way using a standard polarizing microscope, but its presence can be recognized by the typical paramorphotic cholesteric fan texture that is only formed when cooling down from a blue phase. This texture, like that shown in figure 4(*b*), is found for all concentrations above 50 wt % of CN-B-10.

The system, CN-B-10/CN-C-12 (figure 2), is very different from the mixed system shown in figure 1. In this case, a mixture with two chiral components is involved. One compound, CN-B-10, does not show a smectic phase, and the other component, CN-C-12, exhibits cholesteric and smectic phases, but no TGB$_A$ phase. CN-C-12 itself exhibits a monotropic smectic C* phase. This phase is not easy to observe, because, on cooling down, crystallization often occurs before the smectic C* phase is visible. Only in a stream of evaporating liquid nitrogen, could the temperature be decreased fast enough to allow the smectic C* schlieren texture to develop from the homeotropic smectic A phase, in most cases, however, accompanied by crystallization.

On the left-hand side of figure 2, the cholesteric, the broad range smectic A and the monotropic smectic C* phase of CN-C-12 are shown. On the right-hand side, the cholesteric phase of pure CN-B-10 is represented. The smectic A phase exists for all concentrations of CN-C-12 from 10 wt %; only pure CN-B-10 shows no smectic phase. The cholesteric phase exhibited by both pure

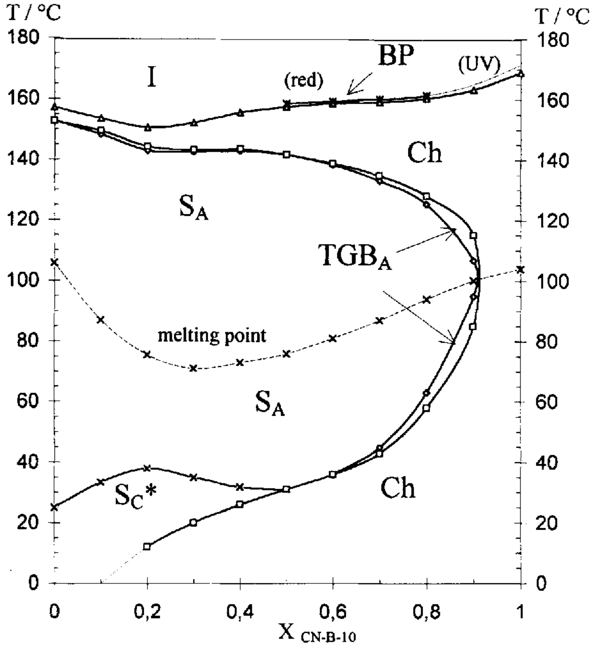

Figure 2. Phase diagram of the mixed system CN-B-10/CN-C-12.

compounds is observed for all mixtures, for those approaching pure CN-C-12 over a range of 5 to 10°C, and for those approaching pure CN-B-10, from a range of 40°C up to that represented by the whole temperature range of the mesophases. The cholesteric phase exists around the smectic A phase, and from 20 to 90 wt % CN-B-10, a re-entrant cholesteric phase is formed. In the region 0 to 50 wt % CN-B-10, the smectic C* phase of CN-C-12 is observable as a grey schlieren texture. In pure CN-C-12, recrystallization occurs very fast, but with 10 to 40 wt % CN-B-10, the smectic C* phase is stabilized with smectic C*–smectic A transition temperatures raised from 25°C up to 40°C. Below the smectic C* phase, the re-entrant cholesteric phase also exists.

In this mixed system, a TGB_A phase is observed around the whole smectic A phase region between the smectic A and cholesteric phases. The TGB_A phase is in fact induced and stabilized for 10 to 90 wt % CN-B-10. It is a broad range TGB_A phase for 10 to 40 wt % and 60 to 90 wt % CN-B-10, but for 50 wt % it is quite narrow. This is caused by the maximum in the transition temperature of the smectic A phase that occurs here around 50 wt % concentration of the compounds, an effect found again in the contact preparations. In this mixed system, the TGB_A phase also exists between the smectic A and the re-entrant cholesteric phases as a re-entrant TGB_A phase that is nicely stabilized in the mixtures from 60 to 90 wt % CN-B-10. For the smectic C*–re-entrant cholesteric transition, a similar effect could exist, as it is possible that this transition could occur via a TGB_C^* phase, but this type of phase is very difficult to identify in the temperature region involved here [10]. For concentrations higher than 40 wt % CN-B-10, a blue phase is observed. At 50 to 80 wt % CN-B-10, a platelet texture is exhibited, again with the concentration-dependent change of the colour of the platelets; at 50 wt % the texture is yellowish and red, and then changes to blue. A blue phase with a pitch in the UV is observed for more than 80 wt % of CN-B-10.

For a better visualization of the observed effects, a series of photomicrographs of the textures formed by the mesophases of the mixed system of figure 2 is shown in figure 3. The mixture of 20 wt % CN-C-12 with 80 wt % CN-B-10 was heated and then cooled down from the isotropic liquid to give the textures illustrated. First the blue phase with its blue platelet texture was observed figure 3 (*a*). From this phase, the cholesteric phase develops showing the typical paramorphotic cholesteric fan texture that is only formed when cooling down from a blue phase, figure 3 (*b*). The same cholesteric texture was found when a blue phase with a pitch in the UV was formed, thereby allowing the indirect detection of the blue phase. (Without a blue phase, the cholesteric texture is completely different; for example, on cooling of a mixture containing 30 wt % CN-C-12 and 70 wt % CN-B-10 the cholesteric fan texture shown in figure 4 is produced.) At lower temperatures, the TGB_A phase with its typical filament texture appears on the black background of the oncoming homeotropic smectic A phase, figure 3 (*c*). The filaments develop from the cholesteric fans, and they still possess the shape and the edges of the fans from which they were formed.

The totally black, featureless, homeotropic smectic A phase is then formed. This persists until the re-entrant TGB_A phase again shows a filament texture, figure 3 (*d*). The filaments have now developed from the homeotropic smectic A phase, and hence no edges or shapes of the precursor fans are shown as in figure 4 (*c*). The re-entrant cholesteric phase that is formed from the re-entrant TGB_A phase shows a small fan texture, figure 3 (*e*), and is different from the cholesteric texture that develops at higher temperatures from a blue phase. In a small area of the picture recrystallization is beginning.

A comparison of figures 1 and 2 shows some similarities. Both mixed systems show a region of smectic A phase that extends close to the pure CN-B-10. In figure 1, the smectic A phase is induced, and in figure 2 the smectic A phase originates from CN-C-12. This shows the ability of CN-B-10 to induce and to stabilize smectic phases (the next member of the homologous series, CN-B-11, forms smectic phases due to its longer terminal chain, and it shows smectic A and TGB_A phases as a pure compound). Both mixed systems possess a

Figure 3 (*a*)

Figure 3 (*b*)

Figure 3 (*c*)

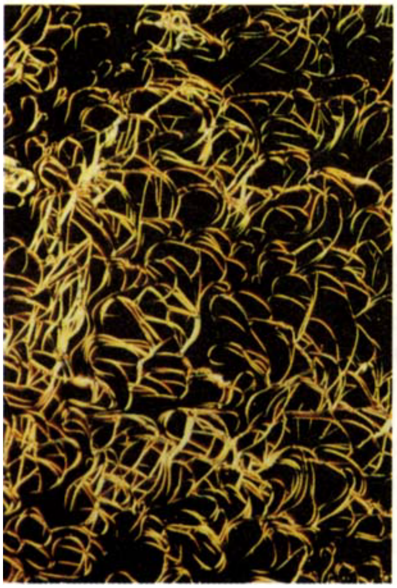

Figure 3 (*d*)

Figure 3 (*e*)

Figure 4

Figure 3. Mixture of 80 wt % CN-B-10 and 20 wt % CN-C-12. Phases occurring on cooling down from the isotropic liquid, 100 ×, crossed nicols: (*a*) blue phase at 159·4°C, platelet texture; (*b*) cholesteric phase at 158·2°C, paramorphotic texture developed from a blue phase; (*c*) TGB_A phase at 125·5°C, filament texture, followed at a lower temperature by the black, featureless texture of the S_A phase—not presented as a photomicrograph; (*d*) re-entrant TGB_A phase at 60·5°C, filament texture; (*e*) re-entrant cholesteric phase at 42·0°C, fan texture, accompanied by crystallization.

Figure 4. Mixture of 30 wt % CN-B-10 and 70 wt % CN-C-12; cholesteric phase at 150°C, developed from the isotropic liquid without a precursor blue phase, 100 ×, crossed nicols.

re-entrant cholesteric phase that exists at higher concentrations of CN-B-10, but only the mixtures of the structurally analogous chiral compounds show a re-entrant TGB_A phase (figure 2). However, both the chiral and the achiral dopant induce a blue phase that is quite sensitive to molecular chirality. The blue phase exists in both cases for concentrations of 50 wt % CN-B-10 and higher, and the change of the pitch of the blue phase induced by an achiral dopant is the same as that caused by a dopant that possesses four chiral centres.

To study further the latent power of the cyano compounds to form and stabilize smectic phases, contact preparations of CN-B-10 and CN-C-12 with compounds having quite a different structure, such as HOPDOB and C7-Chol (see the table) were made. The molten compounds were contacted on the slide and the mesomorphic behaviour along the resulting concentration gradient was observed. The diagrams shown in figure 5 are purely schematic and as they are qualitative, they are not based on distinct molar fractions. The left-hand sides represent 100 wt % of CN-C-12 or CN-B-10.

The phase diagrams show that the induction of smectic and re-entrant phases occurs with quite different compounds. The upper diagrams involving contacts of CN-C-12 with HOPDOB, figure 5 (*a*), and CN-C-12 with C7-Chol, figure 5 (*c*), demonstrate that CN-C-12 forces the development of a re-entrant cholesteric phase which also exists below the stabilized smectic C* phase. The re-entrant cholesteric phase therefore occurs when compounds that do not possess a terminal cyano group that could interact with CN-C-12 are used. The CN-C-12 molecules can only interact via their own cyano groups when mixed with such compounds. The smectic A phase shows in both diagrams a maximum in the smectic A–isotropic transition temperature at nearly 50 wt % concentration of the components. The lower diagrams represent contacts of CN-B-10 with HOPDOB, figure 3 (*b*), and CN-B-10 with C7-Chol, figure 3 (*d*) and show maxima in the smectic A–isotropic transition temperatures at nearly 70 wt % concentration of the dopant. On both sides of the maxima, the cholesteric phase occurs. Only with the chiral dopant C7-Chol is a TGB_A phase formed. These observations show again the latent power of the cyano compounds CN-C-12 and CN-B-10 to form and stabilize smectic phases.

We thank the Deutsche Forschungsgemeinschaft for financial support and Professor G. W. Gray for helpful discussions.

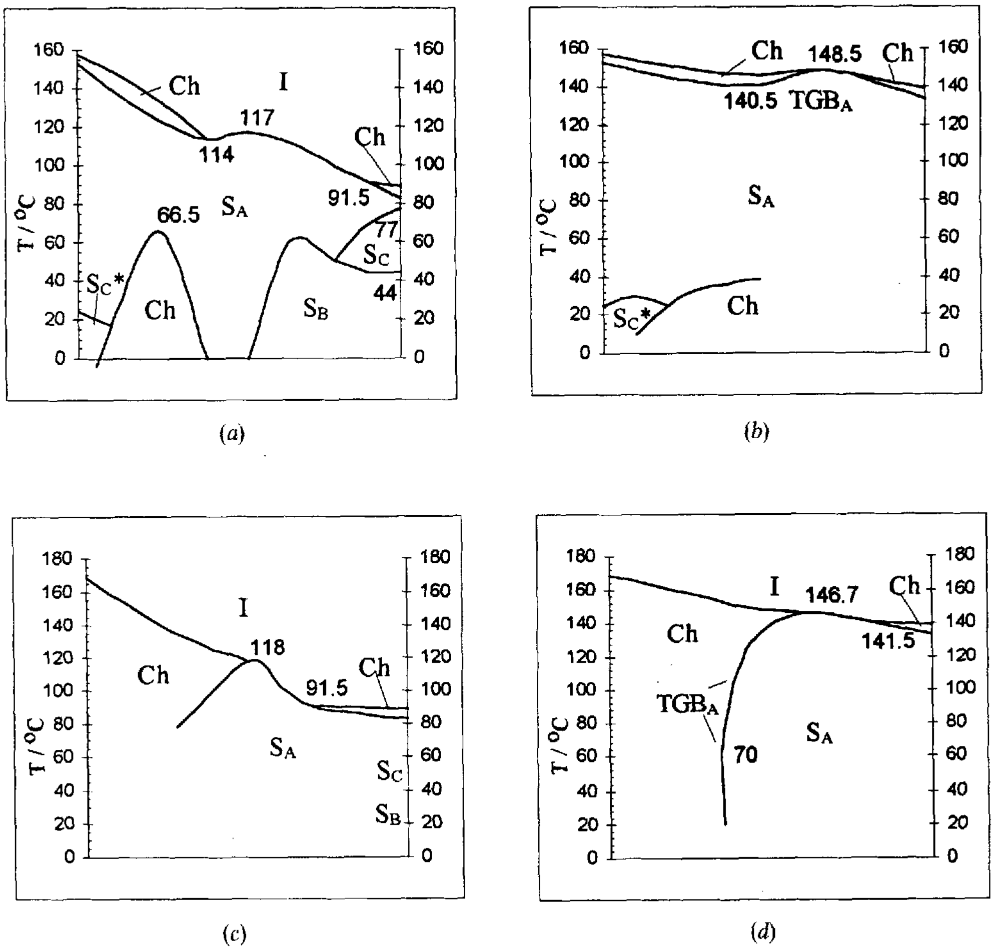

(*a*) (*b*)

(*c*) (*d*)

Figure 5. Phase diagrams of contact preparations: (*a*) CN-C-12/HOPDOB; (*b*) CN-B-10/HOPDOB; (*c*) CN-C-12/C7-Chol; (*d*) CN-B-10/C7-Chol.

References

[1] (a) Goodby, J. W., Waugh, M. A., Stein, S. M., Chin, E., Pindak, R., and Patel, J. S., 1989, *Nature*, **337**, 449; (b) Goodby, J. W., Waugh, M. A., Stein, S. M., Chin, E., Pindak, R., and Patel, J. S., 1989, *J. Am. chem. Soc.*, **111**, 8119.

[2] Madhusudana, N. V., Sadashiva, B. K., and Moodithaya, K. P. L., 1979, *Curr. Sci.*, **48**, 613.

[3] Nguyen, H. T., and Gasparoux, H., 1979, *Mol. Cryst. liq. Cryst.*, **49**, 287.

[4] Destrade, C., Nguyen, H. T., and Malthete, J., 1985, *Mol. Cryst. liq. Cryst.*, **127**, 273.

[5] Vill, V., and Tunger, H.-W., **1995**, *J. chem. Soc., chem. Commun.*, 1047.

[6] Vill, V., Tunger, H.-W., Stegemeyer, H., and Diekmann, K., 1994, *Tetrahedron Asymmetry*, **5**, 2443.

[7] Vill, V., and Tunger, H.-W., **1995**, *Liebigs Ann.*, 1055.

[8] Petrova, M., and Simova, P., 1986, *Cryst. Res. Technol.*, **21**, 959.

[9] Vill, V., Thiem, J., and Rollin, P., 1992, *Z. Naturf.*, **47a**, 515.

[10] Nguyen, H. T., Bouchta, A., Navailles, L., Barois, P., Isaert, N., Twieg, R. J., Maaroufi, A., and Destrade, C., 1992, *J. Phys. II*, **2**, 1889.